ELSEVIER

Polymer 44 (2003) 1949–1956

polymer

www.elsevier.com/locate/polymer

Molecular changes on drawing isotopic blends of polyethylene and ethylene copolymers: 1. Static and time-resolved sans studies

Sandry Coutry, Stephen J. Spells*

Materials Research Institute, School of Science and Maths, City Campus, Sheffield Hallam University, Sheffield S1 1WB, UK

Abstract

Small angle neutron scattering (sans) has been used to observe changes in molecular orientation on deformation of isotopic, melt quenched blends of linear polyethylene and copolymers with butyl and hexyl branches, using uniaxial drawing. In no case was there evidence of significant isotopic fractionation either before or during deformation. Samples left clamped in the neutron beam following deformation showed no evidence of molecular relaxation, while significant changes in molecular orientation with time were observed for samples unclamped after deformation. This latter behaviour could be fitted adequately by a single exponential decay and the relaxation time was found to be of the order of tens of minutes. This relaxation time increased with both increasing molecular weight and the presence of branching. For samples drawn to draw ratios of up to 3.0, the anisotropy in the radius of gyration was compared with predictions for affine deformation. Only in the cases of linear labelled guest molecules in either a linear or copolymer host were significant departures from the affine model observed: no such departures were found for copolymer guest molecules. This is interpreted in terms of a delay in crystallite disruption until higher draw ratios for copolymer guest molecules with respect to linear guest.
© 2003 Elsevier Science Ltd. All rights reserved.

Keywords: SANS; Time-resolved; Drawing

1. Introduction

Many commercial applications of polymers rely on drawn films and fibres, characterised by anisotropic properties. Debate continues on the nature of the deformation process and on the details of the accompanying changes in molecular conformation. Nevertheless, a better understanding of the evolution of molecular conformation would be useful in the improvement of processes, particularly in terms of the range of polymer and copolymer structures now available. Metallocene catalysed polymers have developed a commercial importance over recent years and, with their narrow molecular weight distributions and controllable, homogeneous branch contents, these represent highly suitable materials for fundamental studies of structure in relation to physical properties. In this series of papers, we present infrared and neutron scattering studies of polyethylene (PE) and ethylene copolymer systems under low levels of deformation, with the aim of characterising the changes in molecular conformation. When applied to blends of fully deuterated and undeuterated PE, this combination of experimental techniques provides unique information on the molecular trajectory in the polymer, as has been reviewed elsewhere [1]. The ultimate goal is to clarify the molecular basis for the morphological changes, and hence the physical properties obtained. In this first paper, small angle neutron scattering (SANS) measurements are used to demonstrate differences in the evolution of global molecular conformation with drawing for linear PE blends and blends including ethylene copolymer. The measurements were designed to test the model of affine deformation and to demonstrate the time dependence of molecular relaxation on unclamping a drawn sample. Future papers in the series will examine changes in the infrared spectra with drawing in relation to the SANS data presented here. This will allow changes in local molecular arrangements to be evaluated.

We restrict ourselves here to starting materials crystallised by rapid quenching from the melt: it is well established that this minimises isotopic fractionation in isotopic blends of PE, allowing the full interpretation of SANS data. Previous work by Wignall and co-workers (e.g. [2,3]) has involved the deformation of deliberately isotopically fractionated samples, with major reductions in forward scattering being interpreted in terms of melting and recrystallisation. We chose the approach of minimising

* Corresponding author. Tel.: +44-114-225-3428; fax: +44-114-225-3066.
E-mail address: s.j.spells@shu.ac.uk (S.J. Spells).

0032-3861/03/$ - see front matter © 2003 Elsevier Science Ltd. All rights reserved.
doi:10.1016/S0032-3861(03)00040-5

the initial level of fractionation in order to detect departures from such low levels, using both SANS and mixed crystal i.r. spectroscopic (MCIRS) techniques. While differences in the radius of gyration (R_g) between the molten samples and those quenched from the melt are minor [4,5], small and intermediate angle neutron scattering data have been used to test various models for chain conformation in melt quenched isotopic blends of linear PE. Notably, the 'solidification' [6], 'subunit' [7] and 'variable cluster' [8] models have been proposed. The last two of these involve higher proportions of adjacent re-entry than would be anticipated on the basis of a random arrangement of crystal 'stems' (the individual molecular traverses of the crystal). On incorporating copolymers with either butyl or hexyl branches into isotopic blends, we have recently demonstrated that copolymer guest molecules have a slightly larger proportion of adjacency than linear guests [9]. At the same time, there is a smaller molecular expansion with increasing molecular weight when both guest and host are copolymers.

The combination of elastic neutron scattering and MCIRS has proved invaluable in determining molecular trajectories in PE. Overall molecular dimensions are obtainable from the radius of gyration, using SANS, while the bandshape of the infrared active CD_2 bending vibration allows the local arrangement of crystal stems to be analysed. It should be noted that the CD_2 bending vibration includes doublet components arising from crystal stems as well as a central singlet which includes contributions from both 'isolated' crystal stems (i.e. labelled stems without any labelled {110} neighbours) and amorphous polymer. With knowledge of sample crystallinity, these contributions can be separated. Conversely, the radius of gyration from SANS measurements clearly involves both crystalline and amorphous components of the polymer conformation, without the possibility of their separation. The combined use of neutron scattering and MCIRS has recently been reviewed elsewhere, in relation to melt quenched PE [9]: we simply note here that MCIRS data for slowly cooled linear PE blends indicate around 30–40% of crystal stems in adjacent arrangements [10], while results on melt quenched PE point to a similar proportion [11]. Although the two techniques have not previously been applied to the drawing of PE, it is worth noting that they have been used to study the rolling of linear single crystal blends [12,13]. This allowed the determination of the size evolution of intact crystallite blocks with increasing roll ratio.

In general, the cold drawing of melt quenched PE involves the deformation and final destruction of spherulites and the ultimate formation of a fibre morphology. Characteristics such as the draw ability and the creep resistance of PE are known to be influenced by even a small proportion of short chain branching. This appears to be related to the dependence of spherulite size on both branch length and number [14]. The preferential exclusion of branches from the crystal interior is associated with a decrease in crystallinity, long spacing and lamellar thickness with increasing numbers of branches. It has also been recently proposed that the orthorhombic phase of PE becomes more irregular on deformation [15] and that this disruption is more significant for branched materials. Blends of linear and copolymer PE have previously been studied using SANS, and the results have been reviewed elsewhere [9]. To summarise, at low branch contents (<4 branches per 100 backbone carbon atoms; i.e. larger than the values for samples used here), liquid–liquid phase separation does not occur, although these observations are not in full agreement with conclusions from transmission electron micrographs of surface replicas.

The aim of this series of papers is to characterise the changes in molecular conformation of melt quenched PE during cold drawing and subsequent relaxation. In order to investigate the effects of chain branching, metallocene-catalysed deuterated polymers with homogeneous branch contents are used, alongside linear deuterated polymers of similar molecular weight. The effect of molecular weight was also studied, with pairs of deuterated copolymer and linear materials of 'high' (approx. 400,000) and 'low' (95,000) molecular weight. While the changes in overall dimensions of the fully deuterated 'guest' molecules are studied here using SANS, future papers will focus on analysis of the local molecular reorganisation, based on MCIRS results. The findings will be viewed in the light of morphological evidence, to build a more complete picture of the relationship with the molecular processes involved in deformation. Inevitably, there is a need to restrict the number of variables studied. We restrict ourselves here to relatively low draw ratios ($\lambda \leq 5.0$) and strain rates.

2. Morphological changes and the molecular basis of uniaxial deformation of spherulitic polyethylene

This work concerns the route by which fibre morphology is achieved from a spherulitic starting material. This subject has been reviewed by Porter and Wang [16], who highlighted the features of the process identified by various authors. While different views have been expressed on the steps involved (e.g. [16–18]), it is important to note that we are concerned here with relatively small draw ratios ($\lambda \leq 5.0$), so that the full development of a fibre morphology is not achieved. The initial stages of spherulite deformation are, however, important. Small angle light scattering measurements on PE spherulites during deformation have been interpreted as indicating affine molecular deformation (e.g. [19]). A development of the model by Nomura et al. [20] also incorporated the assumption of an affine deformation, while giving some indication that the development of chain tilt within the lamellae accompanies lamellar untwisting. Measurements by optical microscopy are also important here: Hay and Keller [21] reported

observations on the deformation of a spherulitic film of LDPE. The response was found to be non-uniform and highly recoverable. Deformation was found to take place first in the spherulite radii perpendicular to the draw direction. These regions usually became extensively deformed, mainly through chain slip, while those regions where the radii were at a small angle to the deformation axis were relatively undamaged. More recently, a combination of X-ray diffraction and small angle light scattering has been used to confirm a two step model involving (i) instantaneous spherulitic deformation, including orientation of lamellar axes and lamellar untwisting and (ii) the orientation of crystallites within these lamellae [17].

In terms of understanding the molecular basis of the deformation of PE, extensive studies of the yield behaviour of a range of linear and copolymer samples as a function of parameters such as molecular weight, branch type and concentration and draw temperature were made by Mandelkern and co-workers (e.g. [22–24]). A single curve was found, irrespective of the type of branch, for all types of copolymer, when plotting yield stress versus core crystallinity (obtained from Raman spectroscopy, on the basis of a system with core crystallites, an interfacial region and a liquid-like amorphous phase). This behaviour was found to be independent of molecular weight. Linear polymers show larger yield stresses, in the limited region where their core crystallinities overlap those for copolymers. As for the molecular mechanism for yield, two cases were considered: that of melting and recrystallisation and that involving the thermal activation of dislocations and consequent slip. The first of these cases was suggested by Flory and Yoon [25]. On the basis of their model of highly entangled non-adjacent chain re-entry in melt crystallised polymers, they concluded that cold drawing must result in either chain scission or melting. That melting and recrystallisation occur at sufficiently high draw temperatures is irrefutable (e.g. [2, 3]). However, SANS measurements indicate that this process only occurs above a temperature in the region of 70–90 °C [26]. By considering the thermal activation of screw dislocations with the Burgers vector parallel to the polymer chain direction, the dependence of shear yield stress on crystallite thickness can be calculated. This model failed to give good quantitative agreement with experimental data [23], although it was concluded that some modifications to the theory may provide better agreement.

The deformation of spherulites clearly involves a complex molecular reorganisation. One route to further understanding is to consider a simpler type of initial orientation. This approach was adopted by Adams et al., in a very detailed electron microscopic investigation of oriented thin PE films [27]. A melt drawing method was used to produce thin films with a near-single crystal texture. Despite the differences in morphology by comparison with spherulitic films, this system allowed direct and detailed observation of morphological features at successive stages of drawing, leading to the identification of the sequence:

(1) Separation of lamellae with strain almost entirely accommodated within the interlamellar amorphous regions;
(2) Tie molecules become highly extended and slip is initiated within crystalline lamellae;
(3) Strain-induced crystallisation of the oriented amorphous chains occurs;
(4) Blocks of crystal are pulled out of the lamellae ('block slip');
(5) Portions of lamellae below a critical size decrystallise;
(6) Blocks from crystal shear processes and strain induced crystallisation become aligned along the tensile axis.

Both block slip and fine slip were visually identified and the two slip systems {100} ⟨001⟩ and {010} ⟨001⟩ were distinguished. The sequence described here provides a useful comparison with processes studied in this series of papers.

3. Experimental

Neutron scattering measurements on undeformed samples, using instruments LOQ (ISIS, Chilton, UK) and D11 (ILL, Grenoble, France) are described elsewhere [9]. As previously, D11 was used with a velocity selector providing $\Delta\lambda/\lambda$ of 10%, a wavelength distribution centred at 6 Å and a sample-detector distance of 8 m, while the main ^{3}He detector of LOQ is fixed at 4.05 m from the sample. A Rheometric Minimat tensile tester was used to draw dumbbell-shaped samples of size 1×2 cm. An array of small ink spots was used in conjunction with a travelling microscope to measure the draw ratio at the beam position. The Minimat was mounted on the sample table of either instrument and samples were drawn at a rate of 1 mm min^{-1}. The draw direction was horizontal and the position of the Minimat was adjusted so that the beam passed through the neck region, if appropriate. For measurements on LOQ, a circular beam aperture of diameter 6 mm was used, while for D11 runs a diameter of 5 mm was chosen.

As usual, corrections to raw data were made, using an empty cell and a purely hydrogenous 'blank' sample. Standard software was used for data analysis (Colette for LOQ and rnils, areg and anpolly for D11). For the analysis of anisotropic scattering, sector angles of 30° about horizontal and vertical directions were used to obtain the scattering parallel and perpendicular to the draw direction, respectively. This allows the corresponding radii of gyration, R_{par} and R_{per}, to be calculated [28].

4. Materials

Linear and copolymer PE samples, including metallocene-catalysed materials, were used. These are listed in

Table 1. Linear hydrogenous samples A and B and linear deuterated samples 1, 2 and 3 were kindly supplied by Dr P.J. Barham (University of Bristol), while all the others were produced by BP Chemicals and provided by Dr W. Reed.

Isotopic blending was carried out in solution, using 3 or 5%w/w fully deuterated polymer previously mixed with hydrogenous PE. After precipitation from methanol, the filtered and dried samples were packaged in aluminium and heated to 160 °C in a press for 15 min before quenching into cold water. Films of approximately 0.3 mm thickness were produced in this way. Further details of sample characterisation and preparation are given in Ref. [9].

The sample nomenclature used in Ref. [9] is here extended to include the draw ratio. Hence, for example, CL/95/385/1.3 refers to a blend of a copolymer deuterated PE with molecular weight 95,000 and a linear host PE with molecular weight 385,000, drawn to a draw ratio of 1.3.

5. Results

SANS data for stretched samples were analysed using Zimm plots for scattering in directions parallel and perpendicular to the draw direction. For two samples, LL/95/385 and LC/95/181, the intercepts for wavevector $q = 0$ ($q = 4\pi \sin\theta/\lambda$, where 2θ is the scattering angle and λ the neutron wavelength) were observed to decrease on deformation, corresponding to an increase in forward scattering and an apparent increase in guest molecular weight. This is consistent with isotopic fractionation on deformation as the result of local melting and recrystallisation (e.g. [26]). However, such effects are usually observed for deformation at high temperatures, rather than at room temperature. Furthermore, the apparent molecular weight was never more than twice the value of $\bar{M}_w$ for the undeformed sample. In our case, the evidence for melting and recrystallisation is therefore slight or non-existent.

6. In situ measurements on deformed samples

6.1. Time-dependent measurements

The same sheets of PE blends were used for SANS measurements prior to [9] and after deformation. The small sample mass in the beam following deformation required data collection times of up to 2 h in the case of LOQ runs. It was therefore necessary to determine whether stress relaxation was important over this time scale.

Using instrument D11 at ILL, samples were stretched in the Minimat and then mounted on the sample table before exposing them, at constant strain, to the beam. A data collection time of approximately 30 min was used, with total run times of up to 330 min. Data for 4 samples are shown in Fig. 1: the times shown are elapsed times between the completion of drawing and the middle of each data collection period. The error bars indicated are derived from the least squares fits to successive Zimm plots. While differences between R_{par} and R_{per} demonstrate anisotropy, there is negligible time dependence in either quantity. Hence, stress relaxation does not appear to be a significant effect in clamped samples, at least for elapsed times in excess of around 25 min.

6.2. Evolution of anisotropy with draw ratio

The deformation behaviour of various samples as a function of draw ratio is illustrated in Fig. 2. It was noted earlier [9] that similar values of the radius of gyration, R_g, were obtained using the instruments LOQ and D11. For this reason, data from both instruments are collected here. The radii of gyration measured parallel and perpendicular to the draw direction are shown in Fig. 2, together with power law fits to the data. For an affine uniaxial deformation, if the two directions perpendicular to the draw direction can be taken as equivalent, then

$$R_{affpar} = \lambda R_0 \text{ and}$$
$$R_{affper} = \lambda^{-1/2} R_0 \quad (1)$$

where λ is the draw ratio and R_0 the radius of gyration prior to deformation. R_{affpar} and R_{affper} are the radii predicted

Table 1
Characterisation of polyethylene materials used

Material identifier	Type[a]	$\bar{M}_w(\times 10^{-3})$	$\bar{M}_n(\times 10^{-3})$	$\bar{M}_w/\bar{M}_n$	Side Chain Branches[b]
2	LD	95	48	2.0	–
4	LDM	413	157	2.6	–
5	CDM	95	11	8.6	6.3 C_6
6	CDM	378	181	2.1	8.0 C_4
D	LH	385	48	8.0	–
E	CH	181	15	12.1	6.0 C_4

[a] L denotes a linear polymer; C a copolymer; D a deuterated polymer; H a hydrogenous polymer and M a material polymerised by a metallocene catalysis process.
[b] Number of short chain branches per thousand backbone carbon atoms.

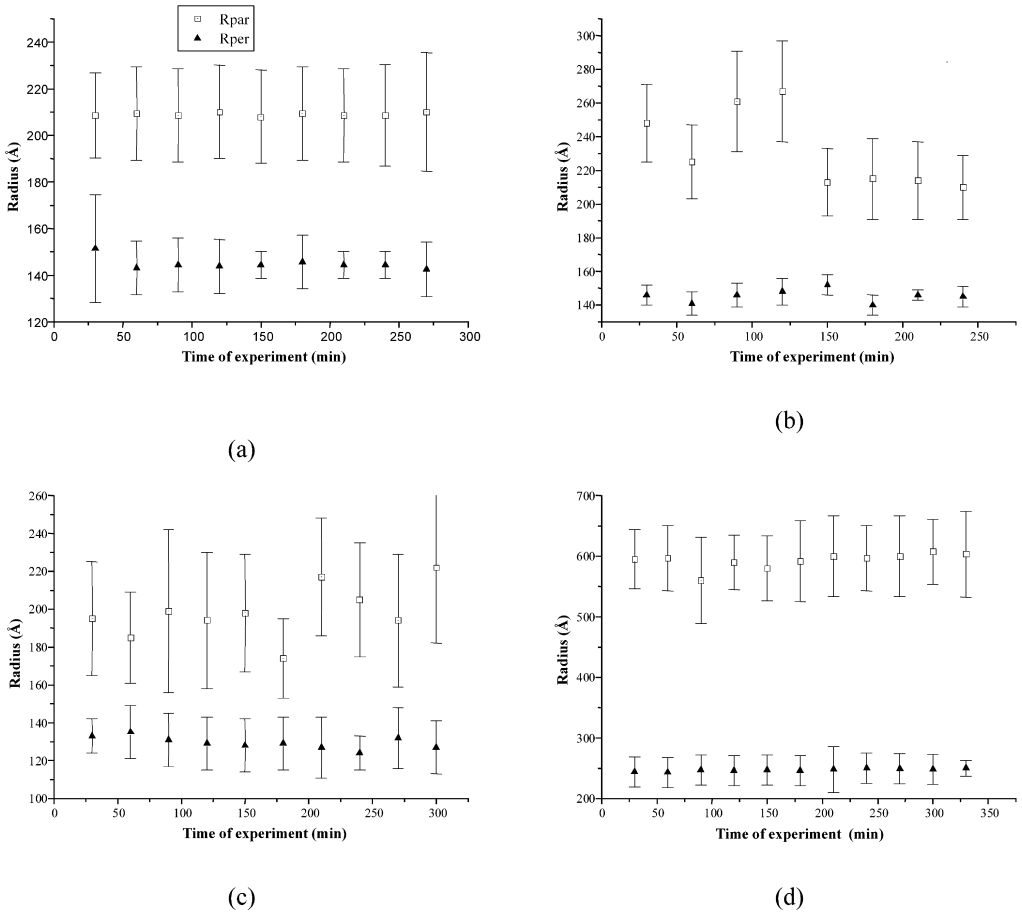

Fig. 1. Evolution of the radii of gyration parallel and perpendicular to the draw direction with time for the sample kept clamped after drawing to a range of draw ratios. The time scale represents the elapsed time following completion of deformation. (a) Sample LL/95/385/1.2; (b) LC/95/181/1.44; (c) CC/95/181/1.5; and (d) LC/413/181/2.33. All measurements were made using instrument D11 at ILL.

parallel and perpendicular to the draw direction. These functions are also plotted in Fig. 2. Representing the power law as

$$R = a\lambda^b \tag{2}$$

the constants a and b can be determined, to compare with the values predicted from Eq. (1) above.

It is clear from Fig. 2 that the evolution of R_{per} with draw ratio seldom shows a significant departure from the affine prediction. Only in two cases—samples LL/95/385 and LC/95/181—do any data points significantly differ from affine values. However, the variation of R_{par} with draw ratio is clearly much more sensitive to departures from affine behaviour. Large deviations are seen in some cases, most notably in those samples with a linear guest species ((a), (c) and (e)), where deviations are significant for draw ratios above about 1.5. The parameters a and b obtained from the least squares fits are listed in Table 2. Values for b_{par} for linear guest DPE samples are significantly smaller than the value of 1.0 expected for an affine deformation. Samples with copolymer DPE yield values of b_{par} which are all less than 1.0, but nevertheless agree with the affine prediction to within the quoted errors.

The distinction between affine and non-affine behaviour is less clear in the values of b_{per}. Two factors can be identified: first the larger fractional errors than for b_{par} and second the constraint imposed by the clamps. This second factor would be significant at low draw ratios. Nevertheless, copolymer guest samples generally show only small departures from the affine prediction of $b_{per} = -0.5$, taking into account the appropriate errors. It is worth noting that the coefficients a_{par} and a_{per} in the power law fits agree in every case, as would be expected.

7. Time-dependent measurements on unclamped deformed samples

Here we investigate the relaxation behaviour of stretched films on removal of constraints. As with previous measurements (above), thin films were drawn using the Minimat tensile tester at 1 mm min^{-1} and ambient temperatures. After stretching to draw ratios of approximately 1.3, the tensile tester was mounted on the sample table and one end of the sample was unclamped. The appropriate region of the sample was then exposed to the neutron beam and data collection periods of around 30 min were used for total run

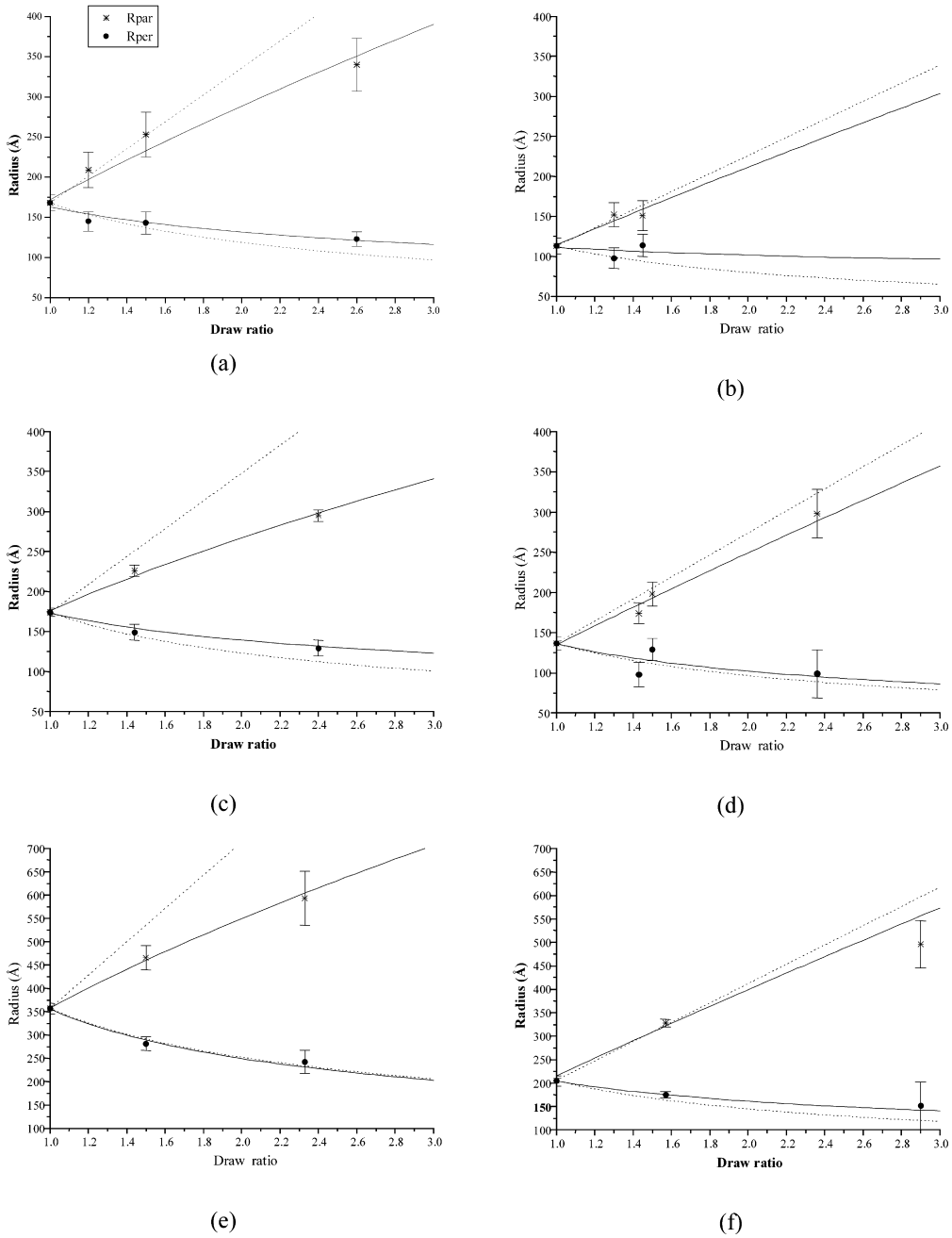

Fig. 2. Evolution of the radius of gyration parallel (×) and perpendicular (●) to the draw direction with draw ratio for samples (a) LL/95/385; (b) CL/95/385; (c) LC/95/181; (d) CC/95/181; (e) LC/413/181; and (f) CC/378/181. The dotted lines represent the expected evolution of R_{par} and R_{per} if the deformation is affine. The solid lines represent the weighted least squares power law fits, of the form $R = a\lambda^b$, on the radii parallel and perpendicular to the draw direction. Measurements were made using instruments LOQ at ISIS and D11 at ILL.

times of up to 240 min. As with the previous data, R_{par} and R_{per} were obtained from each data set. The results are shown in Fig. 3 as a function of elapsed time after unclamping. Unlike the situation with clamped samples, there is clear evidence here for molecular relaxation, following unclamping. A reduction in the ratio R_{par}/R_{per} is observed over the first 60 min or so following unclamping.

Data for different sample types have been analysed on an empirical basis. In all cases, it was found that a single exponential decay could provide an adequate fit to experimental values of the ratio R_{par}/R_{per}, given the large error bars shown in Fig. 3. This can be expressed as

$$\frac{R_{par}}{R_{per}} = \alpha_u + \alpha_r \exp(-t/\tau) \tag{3}$$

where t is the elapsed time after unclamping, τ is a characteristic relaxation time, α_u is the unrecoverable component of R_{par}/R_{per}, representing permanent molecular deformation, and α_r is the recoverable part of R_{par}/R_{per}.

Table 2
Parameters from power law fits on the radii of gyration parallel and perpendicular to the draw direction for the different samples, using data from instruments D11 (ILL) and LOQ (ISIS). a_{par} and b_{par} are obtained from fits on the radius of gyration parallel to the draw direction, while a_{per} and b_{per} relate to measurements perpendicular to the draw direction. For an affine deformation, it is expected that $b_{par} = 1$ and $b_{per} = -0.5$. Results for copolymer guest molecules clearly conform more closely to these predictions

Figure 2	Sample	a_{par}/Å	b_{par}	a_{per}/Å	b_{per}
(a)	LL/95/385	167 ± 3	0.70 ± 0.06	165 ± 3	−0.34 ± 0.06
(b)	CL/95/385	114 ± 8	0.89 ± 0.3	111 ± 8	−0.13 ± 0.32
(c)	LC/95/181	176 ± 4	0.60 ± 0.04	173 ± 4	−0.31 ± 0.05
(d)	CC/95/181	135 ± 7	0.89 ± 0.13	136 ± 8	−0.42 ± 0.22
–	LL/413/385[a]	253	0.57	253	−0.59
(e)	LC/413/181	358 ± 6	0.62 ± 0.05	355 ± 6	−0.51 ± 0.06
(f)	CC/378/181	215 ± 11	0.89 ± 0.11	205 ± 13	−0.34 ± 0.05

[a] No error bars are given for sample LL/413/385 because only one data point was measured (at a draw ratio of 1.39).

Values obtained for the parameters τ, α_u and α_r are listed in Table 3.

8. Discussion and conclusions

The absence of any detectable time dependence in SANS data for samples clamped after stretching indicates that data from clamped samples can be used without the need to consider structural changes related to relaxation. In comparing the radius of gyration components R_{par} and R_{per} with predictions from the affine model, there is a clear difference between linear and copolymer guest molecules, despite the limited range of draw ratio studied here. The linear molecules show departures from affine behaviour at low draw ratios (~ 1.5), while the results for copolymer guest show no significant deviation for draw ratios approaching 3.0. It is reasonable to expect that deformation of amorphous regions—widely accepted to be the first stage in deformation behaviour—may, at least initially, be affine. However, there is no reason to expect that slip processes within crystallites, along with their reorientation, should

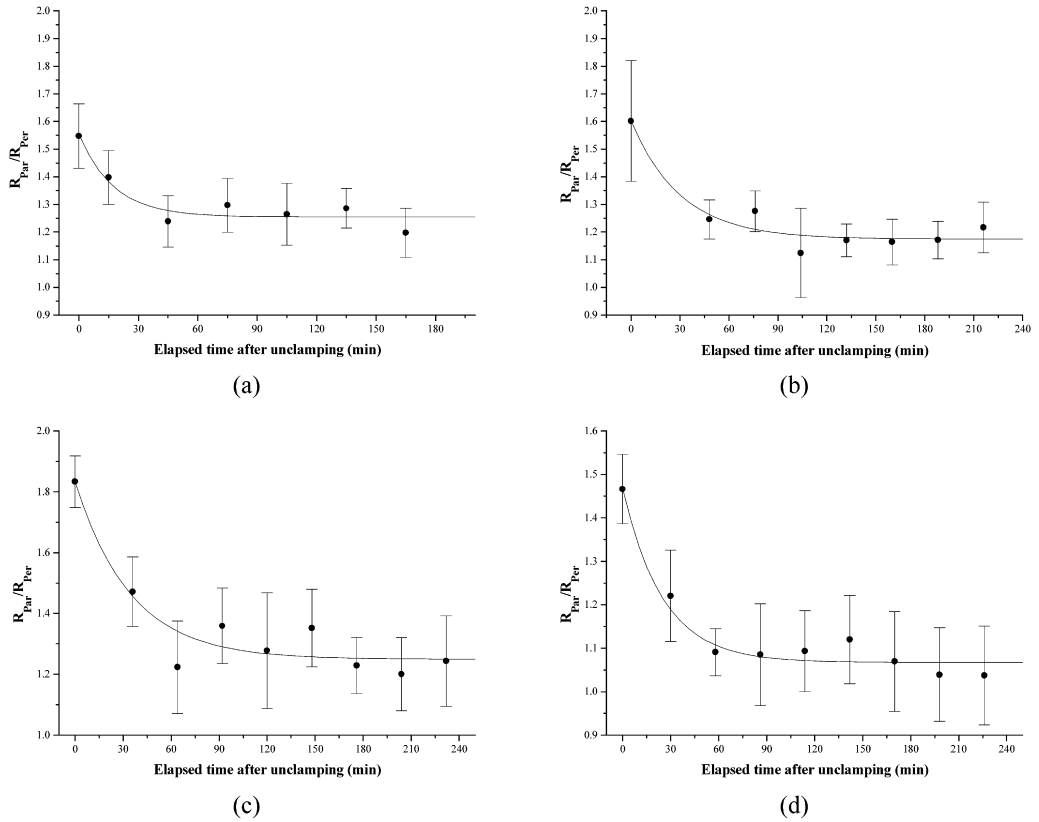

Fig. 3. Evolution of the ratio R_{par}/R_{per} as a function of the elapsed time after unclamping the samples following drawing to a draw ratio of approximately 1.3. Samples: (a) LL/95/385/1.3; (b) CL/95/385/1.3; (c) CC/95/181/1.4; and (d) LL/413/385/1.3. The solid lines represent single exponential decay fits to the data. Measurements were made using instrument D11 at ILL.

Table 3
Results of the single exponential decay fits for the evolution of the ratio R_{par}/R_{per} with elapsed time after unclamping drawn samples. α_u is the permanent component of molecular deformation, α_r is the recoverable component, and τ the characteristic relaxation time

Sample	Draw ratio	α_r	α_u	τ/min
LL/95/385	1.25	0.30 ± 0.06	1.25 ± 0.1	17.5 ± 8
CL/95/385	1.29	0.43 ± 0.05	1.17 ± 0.02	30.5 ± 11
CC/95/181	1.38	0.53 ± 0.05	1.25 ± 0.03	35 ± 10
LL/413/385	1.28	0.40 ± 0.03	1.07 ± 0.02	25 ± 5

result in an affine deformation. As will be shown in later papers, there is evidence that crystal disruption is delayed in the case of copolymer guest molecules. This is consistent with a delay in the onset of non-affine deformation. However, it should be noted that plastic yielding generally occurs well within the range of draw ratios quoted here. Indeed Adams et al., reported lamellar shear occurring at only 50% shear [27]. We can only suggest that, for the copolymer guest molecules used here, orientation of amorphous chains is still the main process.

It is also noteworthy that the pair of extrapolated values of R_0 (represented by a_{par} and a_{per} in Table 2) are in agreement for all samples. This confirms the absence of significant isotopic fractionation during drawing, a conclusion supported by MCIRS results. This in turn shows that melting and recrystallisation is not a major effect under these drawing conditions.

Moving to the measurements during relaxation, if the values for the relaxation time, τ, are first considered without taking into account the associated errors, it can be seen that copolymer guest DPE samples have the largest relaxation times. Increasing the molecular weight of a linear guest DPE molecule within the same linear matrix also results in an increase in relaxation time. If, for sufficiently high molecular weights, entanglements can be considered as effective cross-links, then the chains will relax as fixed end Rouse chains. This implies that, over relatively short time intervals, the relaxation time depends only on the number of monomer units between entanglements. This, in turn, would lead to a relaxation time showing a small dependence on molecular weight. The relaxation times shown in Table 3 are consistent with this view, although the errors in τ are clearly large and effectively limit our confidence in this conclusion. There is certainly no evidence from the behaviour of LL samples to support the reptation prediction of the relaxation time increasing with the cube of the polymer molecular weight. The recoverable component, α_r, shows some dependence on sample type, with copolymer guest DPE samples having slightly higher values than for linear DPE samples. Again, this must be viewed in the light of the errors quoted. Clearly, these experiments with very small sample masses in the neutron beam and relatively short data collection times are on the limits of practicality for the instrument D11. In addition, the earliest evidence of relaxation is lost with initial data collection times of around 30 min.

Acknowledgements

We wish to thank BP Chemicals for supporting SC. We are indebted to Dr Warren Reed (BP Chemicals) and Dr Mary Vickers (University of Cambridge) for valuable discussions and to Dr Mike Dixon (BP Chemicals) for the loan of the Minimat tensile tester. We would also like to thank Dr Steve King (ISIS) and Dr Bruno Deme (ILL) for assistance with neutron scattering experiments.

References

[1] Spells SJ. In: Spells SJ, editor. Characterization of Polid Polymers. London: Chapman and Hall; 1994.
[2] Wu W, Wignall GD, Mandelkern L. Polymer 1992;33:4137.
[3] Annis BK, Strizak J, Wignall GD, Alamo RG, Mandelkern L. Polymer 1996;(37):137.
[4] Schelten J, Wignall GD, Ballard DGH. Polymer 1974;15:682.
[5] Schelten J, Ballard DGH, Wignall GD, Longman G, Schmatz W. Polymer 1976;17:751.
[6] Stamm M, Fischer EW, Dettenmaier M, Convert P. Disc Faraday Soc 1979;68:263.
[7] Sadler DM, Harris R. J Polym Sci, Polym Phys Ed 1982;20:561.
[8] Guttman CM, DiMarzio EA, Hoffman JD. Polymer 1981;22:597.
[9] Coutry S, Spells SJ. Polymer 2002;43:4957.
[10] Jing X, Krimm S. J Polym Sci, Polym Lett Ed 1983;21:123.
[11] Spells SJ. Polym Commun 1984;25:162.
[12] Okoroafor EU, Spells SJ. Polymer 1994;35:4578.
[13] Spells SJ, Okoroafor EU. Polymer 1994;35:4593.
[14] Bubeck RA, Baker HM. Polymer 1982;23:1680.
[15] Lagaron J, Lopez-Quintana S, Rodriguez-Cabello JC, Merino JC, Pastor JM. Polymer 2000;41:2999.
[16] Porter RS, Wang L-H. J Macromol Sci, RMCP 1995;C35:63.
[17] Matsuo M, Xu C. Polymer 1997;38:4311.
[18] Hiss R, Hobeika S, Lynn C, Strobl G. Macromolecules 1999;32:4390.
[19] Clough S, van Aartsen JJ, Stein RS. J Appl Phys 1965;36:3072.
[20] Nomura S, Asanuma A, Suehiro S, Kawai H. J Polym A-2 1971;9:1991.
[21] Hay IL, Keller A. J Mat Sci 1967;2:538.
[22] Failla MD, Mandelkern L. Macromolecules 1993;26:7167.
[23] Kennedy MA, Peacock AJ, Failla MD, Lucas JC, Mandelkern L. Macromolecules 1995;28:1407.
[24] Peacock AJ, Mandelkern L, Alamo RG, Fatou JG. J Mat Sci 1998;33:2255.
[25] Flory PJ, Yoon DY. Nature 1978;272:226.
[26] Sadler DM, Barham PJ. Polymer 1990;31:36.
[27] Adams WW, Young D, Thomas EL. J Mat Sci 1986;21:2239.
[28] Sadler DM. In: Hall I, editor. Crystalline Polymers. London: Applied Science; 1984.